Modeling of vertical axis wind turbine using Ansys Fluent package program

Ismatulla Khujaev[1], *Olimjon* Toirov[2, 3*], *Jura* Jumayev[4], and *Muzaffar* Hamdamov[1]

[1]Institute of Mechanics and Seismic Stability of Structures, Tashkent, Uzbekistan
[2]Tashkent State Technical University, Tashkent, Uzbekistan
[3]Chief Researcher of Institute of Energy Problems of the Academy of Sciences of the Uzbekistan
[4]Bukhara State University, Bukhara, Uzbekistan

Abstract. The paper considers a variant of the problem of modeling the flow around a developed wind turbine. Building a CAD model Fig. 1. was carried out in the SolidWorks environment, where the main geometric dimensions were specified. Since the task is reduced to modeling a flat task, the 2D design mode was chosen.

1 Introduction

In recent years, the Republic of Uzbekistan has adopted a set of measures aimed at further increasing the efficiency of the use of electrical energy in the sectors of the economy and everyday life, the widespread introduction of energy-saving technologies and the development of renewable energy sources [1-3].

Over the past 50 years, 85% of the electricity generation in the republic corresponds to natural gas. The carbon dioxide and carbon oxides emitted from the combustion of hydrocarbons lead to atmospheric pollution, a decrease in its transparency, and an increase in turbidity. This, in turn, amplifies the "greenhouse effect", which over the past hundred years has increased the average temperature of the Earth's atmosphere by 1.5-2 degrees. Such global climate change leads to melting the glaciers of the north and south poles of the Earth and the frequent formation of anomalous climatic phenomena. Ultimately, this is reflected in the planet's global ecological state and civilization's development. In this regard, today, the widespread use of alternative sources of electricity is becoming relevant [4-8].

Of the alternative sources of electricity, the cheapest and most environmentally appropriate is the driving force of the wind, which has a high economic indicator. Based on these considerations, we have developed a prototype wind turbine with a vertical axis, which can operate at low wind speeds and be installed in many regions of the country [9-10].

In general, by 2030, the development of a total wind power capacity of up to 5000 MW is predicted in Uzbekistan.

All this is about big energy. The government also supports small-scale power generation. Evidence of this judgment, in particular, is the financing of this project, which

* Corresponding author: olimjon.t@mail.ru

is aimed at developing and implementing wind turbines with a vertical axis of rotation.

The results of a theoretical study of the aerodynamics of the developed WEG are presented in the last - fourth chapter of the report. Here are the equations for the moving coordinate system; otherwise, it becomes impossible to consider the streamlined body's geometry. The methodology and technology of CFD - computational fluid dynamics and the ANSYS software package are presented. Some results of a computational experiment on the aerodynamics of a wind turbine with a vertical axis of rotation are presented [6-10].

Wind energy is a branch of energy that specializes in converting the kinetic energy of air masses in the atmosphere into electrical, mechanical, thermal, or any other energy that is convenient for use in the national economy. Such a transformation can be carried out by such units as a wind generator, a windmill, a sail, and others [11-26].

In 2019, the total installed capacity of all wind turbines amounted to 651 gigawatts [23] and, thus, exceeded the total installed capacity of nuclear energy (however, in practice, the average annual wind turbine capacity (ICW) used is several times lower than the installed capacity, while Nuclear power plants almost always operate at installed capacity). In 2019, the amount of electrical energy produced by all wind turbines in the world amounted to 1430 terawatt-hours (5.3% of all electrical energy produced by mankind). Some countries are particularly intensive in developing wind energy. According to Wind Europe, in 2019, 48% of all electricity was produced in Denmark with the help of wind turbines, in Ireland - 33%, in Portugal - 27%, in Germany - 26%, in the UK - 22%, in Spain - 21%, in The European Union as a whole - 15% [24, 10-11]. In 2014, 85 countries around the world used wind power on a commercial basis. At the end of 2015, more than 1,000,000 people worldwide are employed in wind energy [3, 11]. Large wind farms are included in the general network; smaller ones are used to supply electricity to remote areas. Unlike fossil fuels, wind energy is virtually inexhaustible, ubiquitous, and more environmentally friendly. However, the construction of wind farms is associated with technical and economic difficulties that slow the spread of wind energy. In particular, the variability of wind flows does not create problems with a small share of wind energy in the total electricity generation; however, with an increase in this share, the problems of the reliability of electricity production also increase [2, 10, 11]. To solve such problems, intelligent control of power distribution is used [6].

In the 16th century, water pumping stations using a hydraulic motor and a windmill began to be built in European cities: Toledo - 1526, Gloucester - 1542, London - 1582, Paris - 1608, and so on.

In the Netherlands, numerous windmills pump water from lands surrounded by dams. The lands reclaimed from the sea were used for agriculture. In arid areas of Europe, windmills irrigated fields [5].

The first wind farm - Blyth's "mill" with a diameter of 9 meters - was built in 1887 at Blyth's country house in Marykirk, UK) [4, 5]. Blyth offered surplus power from his "mill" to the people of Marykirk to light the main street but was turned down because they thought the power was "the work of the devil" [1-4, 5]. Subsequently, Blyth built a wind turbine to supply emergency power to the local hospital, lunatic asylum, and dispensary [4-6]. However, Blyth's technology was deemed not economically viable, and the next wind farm did not appear in the UK until 1951. The first automatically controlled wind turbine by the American Charles Brush appeared in 1888 and had a rotor diameter of 17 meters [10].

In Denmark, the first wind farm was built in 1890, and by 1908 there were already 72 stations with a capacity of 5 to 25 kW. The largest of them had a tower height of 24 meters and four-blade rotors with a diameter of 23 meters. The predecessor of modern horizontal axis wind farms had a capacity of 100 kW and was built in 1931 in Yalta. It had a tower 30 meters high. By 1941, the unit capacity of wind power plants reached 1.25 MW [5-10].

From the 1940s to the 1970s, wind energy experienced a period of decline due to the

intensive development of transmission and distribution networks, which provided energy independent of the weather at moderate prices [10].

A resurgence of interest in wind power began in the 1970s after the 1973 oil crisis. The crisis has demonstrated the dependence of many countries on oil imports and led to the search for options to reduce this dependence. In the mid-1970s, Denmark began testing the forerunners of modern wind turbines. Later, the Chernobyl disaster also stimulated interest in renewable energy sources. California implemented one of the first wind energy incentive programs, starting to provide tax incentives for wind power producers [10].

Currently, the global energy market is in a fever. The conflict between the Russian Federation and Ukraine has given strong metastases throughout the world economy, including in the energy sector. The European economy received about 40% of its energy from the Russian Federation. Today, these paths are gradually closed. In this regard, the green energy movement has been pushed aside. They began to treat the tasks of economic use of energy resources and energy more strictly. Accordingly, interest in the development of renewable energy sources has increased.

Denmark, the Netherlands, and Germany will build an artificial island in the North Sea to generate wind energy. The project is planned to be implemented on the largest shoal of the North Sea - Dogger Bank (100 kilometers from the east coast of England), as the following factors, are successfully combined here: relatively low sea level and powerful air currents. The six-square-kilometer island will have wind farms with thousands of windmills, an airstrip and a port. The main innovation of this construction is the concentration on the lowest possible cost of energy transit. The project's main goal is to create a wind farm that can generate up to 30 GW of cheap electricity. Long-term plans involve increasing this amount to 70-100 GW, providing energy to about 80 million people in Europe, including Germany, the Netherlands, and Denmark [6].

In 2010, 44% of installed wind farms were concentrated in Europe, 31% in Asia, and 22% in North America [10].

In 2014, 39% of electricity in Denmark was generated from wind energy. In 2014, wind farms in Germany produced 8.6% of all electricity produced in Germany [11-15].

According to astronomical climatology, the equatorial part of the Earth heats up more than the polar zones. This fact contributes to the fact that in the equatorial zone, heated and vapor-saturated air begins to move toward the upper layers of the atmosphere. The reason for this is the power of Archimedes. Conversely, the low temperature of the poles causes the air to become heavier, and it tends to decrease. Accordingly, high-pressure zones form near the Earth's surface at the poles, and low-pressure zones are around the equator. A global baric gradient of the surface atmosphere is formed, which, according to the laws of hydromechanics (Berknes' theorem), leads to the formation of a circular motion of air masses: the warm mass moves along the upper layers towards the poles, and the cold mass moves along the surface boundary layer towards the equator. For the northern hemisphere, such a movement of masses is called the arctic wind, and for the southern hemisphere - the antarctic wind and, in general, polar winds. Thus, one can judge the global geostrophic origin of the wind, which can move hundreds and hundreds of tons of moisture in the air circulation.

These flows are comparable in scale to continents and oceans and constitute the global circulation of the atmosphere, which is also known as polar flows. Without considering the Earth's rotation around its axis, these movements of air masses would occur strictly in the direction of the Earth's meridians according to the baric gradient. But the rotation of the Earth around its axis with an angular velocity leads to the formation of the Coriolis force, which forms the western wind (from west to east) of the lower layers of the atmosphere in both hemispheres of the Earth, even ahead of the linear velocity of the Earth's rotation.

In the wind pause (at an altitude of 15-27 km), the thermal component of the air

movement force practically loses its influence, and above it, the east wind already prevails. From this, we can conclude that the masses of the atmosphere, carried away by the general circulation, move along a complex open trajectory, the cause of which is the Coriolis force.

We demonstrate the features of polar flows for the lower layers (up to 15-27 km) of the atmosphere. According to Newton's second law, the acceleration of a mass $1\ м^3$ air with a density ρ is equal to the sum of all forces acting on this mass:

$$\rho\frac{d\vec{U}}{dt}=\vec{G}+\vec{K}+\vec{R}+\vec{P}. \qquad (1)$$

Where

$\vec{U}=u\vec{i}+v\vec{j}+w\vec{k}$ is wind speed vector depending on time and Cartesian coordinates;

$\vec{G}=-\frac{\partial p}{\partial x}\vec{i}-\frac{\partial p}{\partial y}\vec{j}-\frac{\partial p}{\partial z}\vec{k}$ is resulting pressure gradient force;

$\vec{i},\vec{j}$ are unit vectors in horizontal coordinates x, y; $\vec{k}$ are unit vector in vertical coordinate z;

$$\vec{K}=2\rho\left(\omega_z v-\omega_y w\right)\vec{i}+2\rho\left(\omega_x w-\omega_x u\right)\vec{j}+2\rho\left(\omega_y u-\omega_z u\right)\vec{k}= \qquad (2)$$
$$=K_x\vec{i}+K_y\vec{j}+K_z\vec{k}\ -$$

the velocity vector deflecting force of the Earth's rotation is the Coriolis force, defined as $\vec{K}=2\rho\left(\vec{U}\times\vec{\omega}\right)$; $\vec{\omega}=\omega_x\vec{i}+\omega_y\vec{j}+\omega_z\vec{k}$ is the velocity vector of the Earth's rotation around its axis, directed from the south pole towards the north pole;

$$\vec{R}=\frac{\partial}{\partial z}(\eta+A)\frac{\partial u}{\partial z}\vec{i}+\frac{\partial}{\partial z}(\eta+A)\frac{\partial v}{\partial z}\vec{j}+\frac{\partial}{\partial z}(\eta+A)\frac{\partial w}{\partial z}\vec{k} \qquad (3)$$

– resultant of all molecular stresses η and turbulent A friction force;

$\vec{P}=\rho g\vec{k}$ – gravity;

$$\frac{d\vec{U}}{dt}=\left(\frac{\partial u}{\partial t}+u\frac{\partial u}{\partial x}+v\frac{\partial u}{\partial y}+w\frac{\partial u}{\partial z}\right)\vec{i}+\left(\frac{\partial v}{\partial t}+u\frac{\partial v}{\partial x}+v\frac{\partial v}{\partial y}+w\frac{\partial v}{\partial z}\right)\vec{j}+ \qquad (4)$$
$$+\left(\frac{\partial w}{\partial t}+u\frac{\partial w}{\partial x}+v\frac{\partial w}{\partial y}+w\frac{\partial w}{\partial z}\right)\vec{k}\ -$$

substitutionary derivative of the velocity vector, which considers the velocity vector's variability in coordinates: the first terms in brackets are the local components of the acceleration vector, and the next three are the convective components of the acceleration vector.

The system of equations (1), which consists of three equations, is usually supplemented by the atmosphere continuity equation

$$\frac{\partial \rho}{\partial t}+\frac{\partial(\rho u)}{\partial x}+\frac{\partial(\rho v)}{\partial x}+\frac{\partial(\rho w)}{\partial z}=0. \qquad (5)$$

and is closed by the equation of the state of the atmosphere in the form $p(x,y,z,t)=f(\rho x,y,z,t)$.

Such interpretation of the components of the vector equation (1) and the continuity equation refers to the Cartesian coordinate system. For weather forecasting, geographic or spherical coordinates can be used, with additional equations for temperature (energy) and precipitation.

In simplified versions of the calculation in Cartesian coordinates, the most interesting is the horizontal component of the Coriolis force $\vec{K}_s$. This considers that the vertical component of the velocity vector is one hundred and thousand times less than the horizontal components. In this regard, one can take $K_x=2\rho\omega_z v,\ K_y=-2\rho\omega_z u.$ Then only the horizontal component of the Coriolis force is taken into account in the calculations

$$K_s=\sqrt{K_x^2+K_y^2}=2\rho\omega_z U\cdot \qquad (6)$$

where $\omega_z=\omega\sin\varphi$ is vertical component of the angular velocity of the Earth's rotation, $\omega=2\pi/(78400\,c)$ is cyclic frequency of the Earth's rotation around its own axis; φ is geographic latitude of the area; $U=\sqrt{u^2+v^2}$ is wind speed in this simplified approach.

In this case, if the direction of the wind corresponds to the direction of the axis, then the component of the Coriolis force is directed to the right in the northern hemisphere and to the left in the southern hemisphere of the Earth, i.e., $\angle(\vec{U},K_s)=90^0$ – the angle between the velocity vector and the Coriolis force is 90^0 .

The calculations consider the molecular η and turbulent A dynamic viscosities of the atmosphere. According to the provisions of the turbulent boundary layer, only in a thin viscous layer does molecular viscosity play a significant role.

Thus, in a simplified version of the calculation, equations (1) are written relative to the air mass acceleration and take the form

$$\begin{cases}\rho\dfrac{du}{dt}=-\dfrac{1}{\rho}\dfrac{\partial p}{\partial x}+2\rho\omega_z v+\dfrac{\partial}{\partial z}(\nu+k)\dfrac{\partial u}{\partial z},\\ \rho\dfrac{dv}{dt}=-\dfrac{1}{\rho}\dfrac{\partial p}{\partial y}-2\rho\omega_z u+\dfrac{\partial}{\partial z}(\nu+k)\dfrac{\partial v}{\partial z},\\ -\dfrac{\partial p}{\partial z}=g\rho,\quad \dfrac{\partial \rho}{\partial t}+\dfrac{\partial(\rho u)}{\partial x}+\dfrac{\partial(\rho v)}{\partial x}=0.\end{cases} \qquad (7)$$

where $\nu,\ k$ are kinematic coefficients of molecular and turbulent viscosity.

At altitudes of 50-1500 (100-1500) meters, turbulent dynamic viscosity is hundreds and thousands of times higher than molecular viscosity. And at altitudes over 1500 meters (free atmosphere), the role of friction is insignificant because the value of the vertical velocity

gradient is small, and the movement of the atmosphere is determined by the pressure force, the Coriolis force, and the centrifugal force.

There are options for considering the formation of thermals, which, depending on their composition (density) and initial temperature, rise up through the atmosphere, forming peculiar mushrooms [12].

With dynamic changes in the state of the atmosphere, a low-pressure zone (cyclones) and a high-pressure zone (anticyclones) are formed. In the northern hemisphere, in a steady cyclone, the air moves counterclockwise along the isobars, and in an anticyclone, clockwise. In the southern hemisphere, reverse directions of movement are observed under the influence of the Coriolis force. The movement of air under the influence of a cyclone and an anticyclone occurs not only in the direction of the direction difference but also, under the influence of the Coriolis force, performs an additional rotational movement.

When solving simplified equations (i.e., flows in a plan), one usually passes to new sought-for functions, introducing the function of the stream and the vortex. Various methods for the numerical solution of such a system of equations are given in books on methods for solving problems of heat and mass transfer [15–19] and computational fluid dynamics [15–19].

When considering the surface layer (0-50 to 0-100 m), the equations of motion of air masses are simplified. In particular, the equations

$$k\rho\frac{dU}{dz}=\tau_0,\ \frac{u}{v}=tg\alpha=const \tag{8}$$

with an error of 10% will ensure the accuracy of describing the state (movement) of air masses. Here $U=\sqrt{u^2+v^2}$; τ_0 is tension between the surfaces of the layers of the atmosphere; α is angle of deviation of the wind direction from the isobar; coordinate *x* is along the tangential isobar, coordinate *y* is normal to the isobar.

The turbulence coefficient for the surface layer can be taken according to L. Prandtl (1932)

$$k=l^2\frac{dU}{dz} \tag{9}$$

where l is the length of the mixing path of the moles (scale of turbulence).

With the involvement of friction speed (or dynamic speed) $u_*=\sqrt{\tau_0/\rho}$ and assumptions $l=\varpi\left(z+z_0\right)$ $\varpi=0.38$ is Karman's constant; z_0 is characteristic value on the Earth's surface), you can get a formula for the distribution of air velocity over height

$$U\left(z\right)=\frac{u_*}{\varpi}\ln\frac{z+z_0}{z_0} \tag{10}$$

If for a certain height z_3 (1 m from the surface of the Earth, the height of the weather vane, or 30-meter height), the value of the speed is known

$$U\left(z_3\right)=\frac{u_*}{\varpi}\ln\frac{z_3+z_0}{z_0} \tag{11}$$

then it becomes a dependency

$$U\left(z\right)=c_3\ln\frac{z+z_0}{z_0}/\ln\frac{z_3+z_0}{z_0}. \tag{12}$$

This formula for the distribution of air velocity along the height allows you to obtain the dependence for the turbulence coefficient in the surface layer

$$k\left(z\right)=c_3\varpi^2\left(z+z_0\right)/\ln\frac{z_3+z_0}{z_0}, \tag{13}$$

which expresses the linear increase in the turbulence coefficient $\left(k\left(z\right)=k_0+\beta z\right)$ height of the surface layer of the atmosphere.

They gave an example of a simple L. Prandtl model. Research is intensively continuing to adequately describe the flow turbulence in technological installations and nature. We will return to them below in a separate section of the report.

At present, quite complex mathematical models and supercomputers are used for weather forecasting.

Numerous results of theoretical testing of wind turbines have been produced in the ANSYS Fluent software package. Some works have been done in MATLAB [13] and other software packages. Many commercial CFD software products are used in engineering, such as PHOENICS (the first commercial CFD software), STAR-CD, ANSYS FLUENT/CFX, and so on. All CFD software products have three main structures: Pre-Processer, Solver, and Post Processor [14, 22-23]. But the essence of solving aerodynamics problems in all cases is the answer to the question: what aerodynamic forces are formed when solving an external problem.

2 Materials and methods

The paper considers a variant of the problem of modeling the flow around a developed wind turbine.

Building a CAD model Fig. 1. was carried out in the SolidWorks environment, where the main geometric dimensions were specified. Since the task is reduced to modeling a flat task, the 2D design mode was chosen.

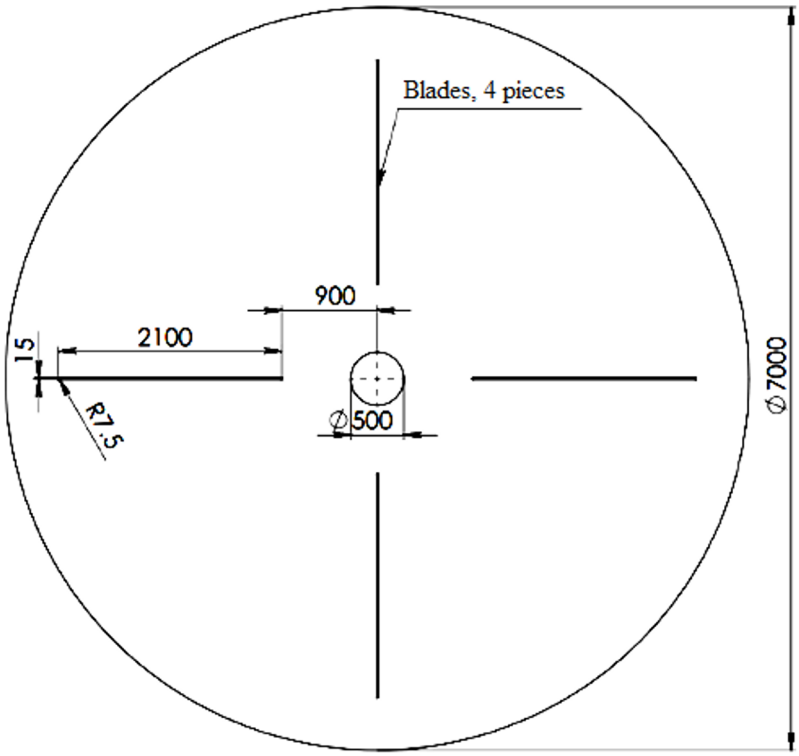

Fig. 1. 2D wind turbine geometry (top view)

In solving the problem, one turbulence model can be used to describe turbulence.
Model modified $\boldsymbol{k-\varepsilon}$. In contrast to the well-known works, it is proposed here to describe the turbulent exchange using a modified $k-\varepsilon$ model, which contributes to an adequate description of the heat and mass transfer process:

$$\begin{cases} \dfrac{\partial}{\partial t}(\rho k)+\dfrac{\partial}{\partial x_j}(\rho k u_j)=\dfrac{\partial}{\partial x_j}\left[\left(\mu+\dfrac{\mu_t}{\sigma_k}\right)\dfrac{\partial k}{\partial x_j}\right]+G_k+G_b-\rho\varepsilon-2\rho\varepsilon M_t^2+S_k, \\ \dfrac{\partial}{\partial t}(\rho \varepsilon)+\dfrac{\partial}{\partial x_j}(\rho \varepsilon u_j)=\dfrac{\partial}{\partial x_j}\left[\left(\mu+\dfrac{\mu_t}{\sigma_\varepsilon}\right)\dfrac{\partial \varepsilon}{\partial x_j}\right]+\rho C_1 S\varepsilon-\rho C_2\dfrac{\varepsilon^2}{k+\sqrt{\nu\varepsilon}}+C_{1\varepsilon}\dfrac{\varepsilon}{k}C_{3\varepsilon}G_b+S_\varepsilon. \end{cases}$$

Here we use the notation

$$C_1=\max\left[0.43,\frac{\eta}{\eta+5}\right],\ \eta=S\frac{k}{\varepsilon},\ S=\sqrt{2S_{ij}S_{ij}},\ \mu_t=\rho C_\mu\frac{k^2}{\varepsilon},\ C_\mu=\frac{1}{A_0+A_S\dfrac{kU^*}{\varepsilon}},$$

$$U^*\equiv\sqrt{S_{ij}S_{ij}+\tilde{\Omega}_{ij}\tilde{\Omega}_{ij}},\quad \Omega_{ij}=\overline{\Omega_{ij}}-2\varepsilon_{ijk}\omega_k,\quad A_S=\sqrt{6}\cos\phi,\quad \phi=\frac{1}{3}\cos^{-1}\left(\sqrt{6}W\right),$$

$$W = \frac{S_{ij}S_{jk}S_{ki}}{\tilde{S}^3},\ \tilde{S} = \sqrt{S_{ij}S_{ij}},\ S_{ij} = \frac{1}{2}\left(\frac{\partial u_j}{\partial x_i} + \frac{\partial u_i}{\partial x_j}\right),\ G_k = -\rho\overline{u_i'u_j'}\frac{\partial u_j}{\partial u_i},\ S \equiv \sqrt{2S_{ij}S_{ij}},$$

$$G_b = \beta g_i \frac{\mu_t \partial T}{\Pr_t \partial x_i}, \qquad \Pr_t = 1/a_t \quad , \quad a_0 = 1/\Pr = k/\mu c_p, \qquad \beta = -\frac{1}{\rho}\left(\frac{\partial \rho}{\partial T}\right)_p,$$

$$G_b = -g_i \frac{\mu_t}{\rho \Pr_t}\frac{\partial \rho}{\partial x_i},\ M_t = \sqrt{\frac{k}{a^2}},\ a = \sqrt{\gamma RT}.$$

Empirical Constants $k-\varepsilon$ models [20-21] take standard values: $C_{1\varepsilon} = 1.44, C_2 = 1.9$, $\sigma_k = 1.0$, $\sigma_\varepsilon = 1.2$, $A_0 = 4.04$.

3 Results and discussion

Calculation grid. Next, the CAD model was exported to Cadence Pointwise to create a hybrid finite volume mesh (Figure 2). An O-grid topology type was chosen to define the CFD flow domain. The input velocity boundary condition was specified in the I first quarter of the circular domain and in the remaining parts of the atmospheric pressure output condition. Also, cell layers were allowed directly at the blade walls to accurately model the turbulent viscous layer, where $Y+ < 4$.

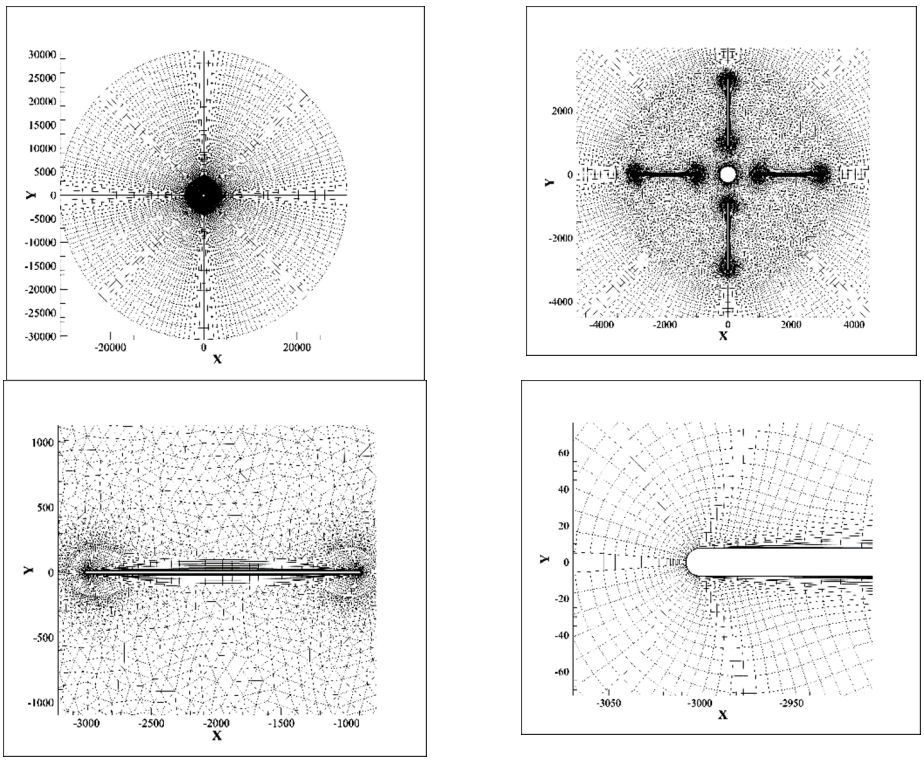

Fig. 2. Unstructured computational grid of finite volumes.

Type - unsteady incompressible flow in 2D formulation. The mass of the installation is 68 kg, the moment of inertia along the Z axis is 85 kg·m2. Input speed -.
The results of modeling the rotation of the wind turbine blades showed a speed of 20-25 rpm with a wind speed of 5 m/s (see Figure 3).

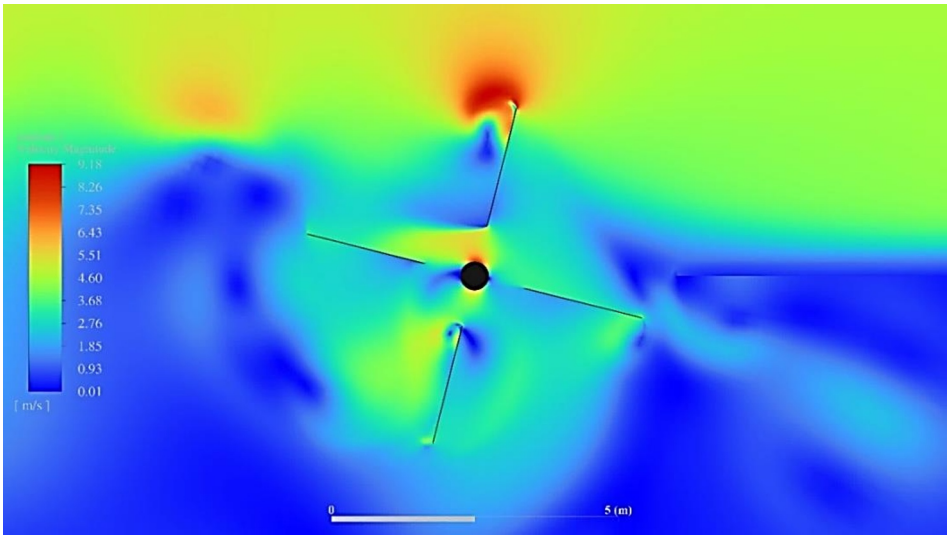

a)

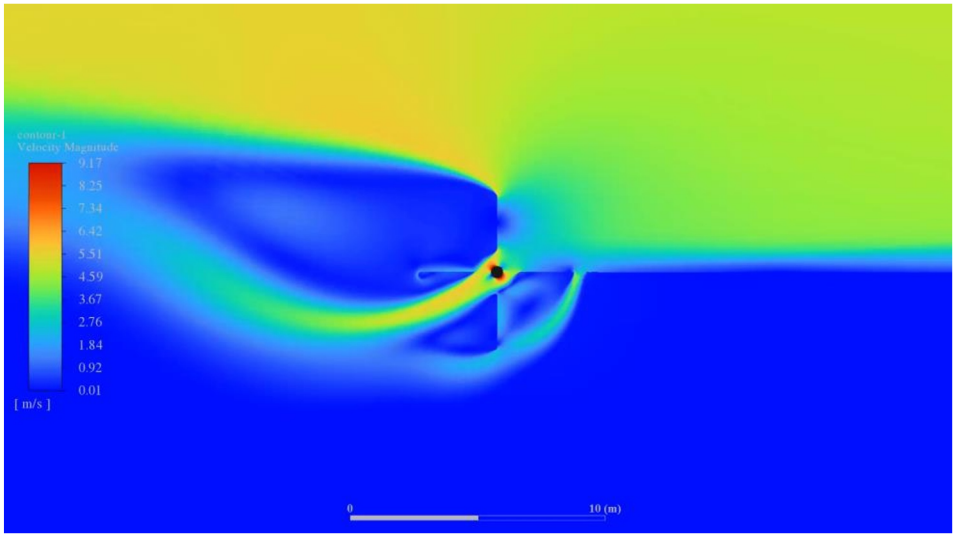

b)

Fig. 3. Speed Loop *V=5 m/s*

According to the preliminary experimental results, the power curve of the installation was plotted depending on the wind speed (Figure 4).

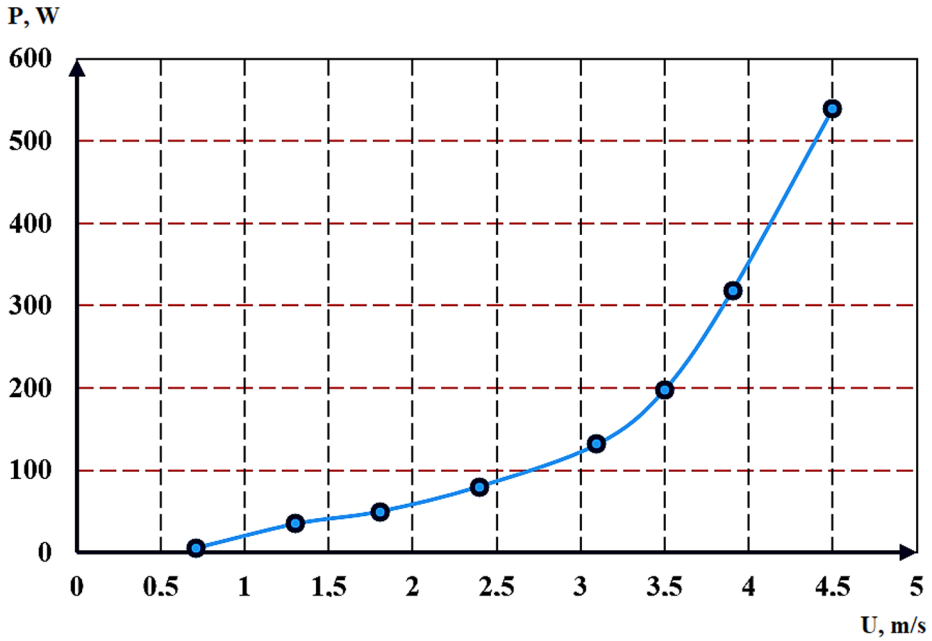

Fig. 4. Power Curve

4 Conclusion

The history and state of the use of wind energy in the world and individual countries have been studied. The total power of the WEG is gradually increasing. Cases of earth-scale wind formation and local winds are highlighted.

In the Republic of Uzbekistan, work is underway on the use of wind energy. The construction of the Tamdy wind farm has begun, and the construction of wind farms in the Bukhara region and the Republic of Karakalpakstan is planned. Scientific and practical work is underway to develop and operate low-power VEGs.

The existing forms of VEG blades with vertical and horizontal axes of rotation are analyzed. It has been found that VEGs with a vertical axis of rotation have the possibility of increasing the usable working area and the advantages of being independent of the wind direction.

Numerous results on the aerodynamics of the HTBO have been obtained, which should be further processed by statistical methods and analyzed.

Theoretical calculations in the ANSYS environment have established that when calculating the aerodynamics of the proposed HTTO, one can use turbulence models $k-\omega$, which more adequately describe the flow process around a rotating device.

Primary experimental results have been obtained, showing that at wind speeds above 4 m/s, the developed device can provide 0.5 kW of energy.

The results on the aerodynamics of the HTBO, which are not included in this report, must be further processed by statistical methods and analyzed.

References

1. Global Wind Report 2019 | Global Wind Energy Council.
2. Wind energy in Europe in 2019, Wind Europe, P. 18-19 (2020).
3. GWEC lauds 1.1 million workers in wind, GWEC.
4. Ponyatov A. Having entered the era of electricity, Science and life, No. 1, P. 16 (2020).
5. Alan Wyatt, Electric Power: Challenges and Choices, Book Press Ltd., Toronto, ISBN 0-920650-00-7 (1986).
6. Gostintsev Yu.A., Yodgorov O.O., Fayziev R.A. (Lazarev VV) Turbulent jet streams in a stratified atmosphere. Preprint in 2 parts. Chernogolovka, 87 p (1989).
7. Obukhov S.G., Sarsikeev E.Zh. Mathematical model of a small wind turbine in MATLAB SIMULINK, International Scientific Journal "Alternative Energy and Ecology" (ISJAEE), No. 02(106), P. 42-48 (2012).
8. Paskonov V.M., Polezhaev V.I., Chudov L.A. Numerical modeling of heat and mass transfer processes, M.: Nauka, 288 p (1984).
9. Roach P. Computational fluid dynamics, M.: Mir, 616 p (1980).
10. Anderson D., Tannehill J., Pletcher R. Computational fluid mechanics and heat transfer: In 2 volumes. Per. from eng, M.: Mir, P. 728 (1990).
11. Patankar S. Numerical methods for solving problems of heat transfer and fluid dynamics. Translated from English, M.: Energoatomizdat, 152 p (1984).
12. Basarab M.A. Numerical-analytical method for solving two-dimensional problems of natural convection in closed cavities, Mathematical modeling and numerical methods, No. 1, P. 18–35 (2014).
13. Hamdamov M.M. Simulation and modeling of flow field around a horizontal axis wind turbine. ICISCT 2022 conference is technically sponsored, IEEE photonics society. (2022).
14. Hamdamov M.M., Ishnazarov A.I., Mamadaliev Kh.A. Numerical modeling of vertical axis wind turbines using Ansys Fluent software, NEW2AN 2022: the 22nd International Conference on Next Generation Wired/Wireless Networks and Systems, Uzbekistan, (2022).
15. Hadha Afrisal, Ahmad Didik Setiyadi, Munawar Agus Riyadi, Rifky Ismail, Iwan Setiawan, *International Journal on Advanced Science, Engineering and Information Technology*, Vol. 12 (2022) No. 6, p. 2258-2265, DOI:10.18517/ijaseit.12.6.16591
16. Olimjon Toirov, Sardor Urokov, Utkir Mirkhonov, Hadha Afrisal, Dilnoza Jumaeva, *E3S Web of Conferences,* SUSE-2021, **288**, 01086 (2021).
17. Olimjon Toirov, Kamoliddin Alimkhodjaev, Akhror Pardaboev, *E3S Web of Conferences,* SUSE-2021, **288**, 01085 (2021).
18. Olimjon Toirov, Dilnoza Jumaeva, Utkir Mirkhonov, Sardor Urokov, Shakhboz Ergashev, AIP Conference Proceedings **2552,** 040021 (2023).
19. Nurali Pirmatov, Allabergen Bekishev, Najmiddin Kurbanov, Oliyakhon Zaynieva, Usmon Norkulov, *AIP Conference Proceedings* **2552**, 040020 (2023).
20. Dilnoza Jumaeva, Akmal Abdurakhimov, Khodjiakbar Abdurakhimov, Nigora Rakhmatullaeva, E3S Web of Conferences, **288**, 01082 (2021).
21. Dilnoza Jumaeva, Zuhriddin Okhunjanov, Umidjon Raximov, Rano Akhrorova. *Journal of Chemical Technology and Metallurgy*, **58,** 2, 2023, 353–359.
22. Olimjon Toirov, Salikhdjan Khalikov, E3S Web of Conferences **377**, 01004 (2023).

23. Adel Aljwary, Ziyodulla Yusupov, Rustam Shokirov, E3S Web of Conferences, **304**, 01010 (2021).
24. Dilnoza Jumaeva, Nigora Rakhmatullaeva, Ravshan Akhmedov, Izzat Eshmetov, E3S Web of Conferences, **288**, 01041 (2021).
25. Toirov O., Khalikov S. E3S Web of Conferences **365,** 04010 (2023).
26. Toirov O., Khalikov S. Diagnostics of pumping units of pumping station of machine water lifting, E3S Web of Conferences **365**, 04013 (2023).